Available online at www.sciencedirect.com

ScienceDirect

Procedia CIRP 75 (2018) 103–107

www.elsevier.com/locate/procedia

15th CIRP Conference on Computer Aided Tolerancing – CIRP CAT 2018

# Data fusion methods for statistical process monitoring and quality characterization in metal additive manufacturing

Marco Grasso*, Francesco Gallina and Bianca Maria Colosimo

*Department of Mechanical Engineering, Politecnico di Milano, Via La Masa 1, 20156 Milano, Italy*

* Corresponding author. Tel.: +39 02 2399 8560; fax: +39 02 2399 8585. *E-mail address:* marcoluigi.grasso@polimi.it

**Abstract**

Metal additive manufacturing (AM) technologies enable the production of complex shapes, lightweight structures and novel functional features. Such increased complexity of the products imposes various challenges in terms of statistical process monitoring and quality assessment. However, one great potential of AM processes, compared to conventional ones, consists of the possibility of gathering a large amount of data layer by layer. This study investigates a data fusion methodology to combine in-situ data from multiple sensors embedded in Electron Beam Melting (EBM) systems to automatically detect faults and process errors. The aim consists of making sense of information already available from the system to enhance its embedded intelligence via novel data mining techniques. A real case study in EBM is presented and discussed.


Peer-review under responsibility of the Scientific Committee of the 15th CIRP Conference on Computer Aided Tolerancing - CIRP CAT 2018.

*Keywords:* Electron beam melting; data fusion; statistical process monitoring; support vector machine.

## 1. Introduction

The industrial use of metal powder bed fusion (PBF) processes has been continuously growing in the last years, especially in the aerospace and bio-medical sectors, where they provide brand new capabilities with respect to conventional processes. Despite of this, several sources of process instability and various kinds of defects may lead to high scrap fractions. The most common defects include internal and surface porosity, cracks and delaminations, residual stresses, dimensional and geometrical distortions, impurities and deviations from the expected microstructure [1-5]. Because of this, most metal PBF system developers have been integrating sensors for in-situ data acquisition and process monitoring [3]. There is also a rapidly growing literature devoted to in-situ process monitoring techniques based on different sensing configurations [7 – 31]. Generally speaking, laser-PBF processes may be monitored via co-axial sensors (i.e., sensors installed within the optical path of the laser) and off-axis sensors (i.e., sensors placed outside the optical path) [1, 3, 30 - 31]. In electron beam-PBF (a.k.a. Electron Beam Melting- EBM), instead, only off-axis configurations are available, because the energy source is an electron beam deflected by electro-magnetic coils, which prevents from using co-axial sensing [1]. In the mainstream literature devoted to EBM process monitoring [3], off-axis infrared (IR) cameras represent the major source of information. [34] used IR vision to characterize the surface pattern of scanned slices to detect flaws and surface defects. [35] and [38] used IR vision for surface pattern and geometry characterization of molten slices, whereas the temperature distribution over the entire build area was studied by [36 - 37]. [32] and [33], instead, used video imaging to monitor the evolution of thermal patterns during the EBM process.

However, EBM systems are also equipped with a large number of embedded sensors to monitor the vacuum chamber environment, the energy source and different subsystems. Currently, those sensor signals are not used for monitoring purposes, but they enclose a large amount of relevant

2212-8271 © 2018 The Authors. Published by Elsevier B.V.
Peer-review under responsibility of the Scientific Committee of the 15th CIRP Conference on Computer Aided Tolerancing - CIRP CAT 2018.
10.1016/j.procir.2018.04.045

information about the process and the occurrence of undesired events.

Differently from previous studies based on external IR cameras, the goal of this study consists of proposing a novel data mining approach to fuse together information from sensors that are already embedded in the system, in order to determine the process stability and to anticipate the detection of out-of-control behaviors that may affect the final quality of the part. To this aim, a statistical learning method based on the Support Vector Machine (SVM) formalism [39] is proposed and combined with a control charting scheme applied to multiple sensor data streams. The proposed approach is aimed at detecting defects and process faults that can be related to the stability of embedded signals. This includes defects caused by errors in the powder deposition, unstable beam behaviors, so-called smoking phenomena [3] that alter the environmental conditions, etc. This study specifically deals with an out-of-control state corresponding to a geometrical distortion of the part caused by a wrong powder deposition. Such defect is among the ones that can be detected online via the proposed approach as various signals related to the recoating behavior and the dosing in each layer are available from embedded sensors. However, those signals provide only indirect information about the occurrence of geometrical defects. To further improve the capability of detecting this kind of defects during the process, a data fusion approach that integrates embedded signals with in-situ imaging is needed. This is will be the subject of a future work. In this study, a real case in EBM of Ti6Al4V parts produced either under in-control and out-of-control conditions is presented. Section 2 introduces the real case study and the signals available from embedded sensors. Section 3 briefly described the proposed methodology. Section 4 presents the results and Section 5 concludes the paper.

## 2. Real case study

The real case study consists of the production of a test artifact via EBM of Ti6Al4V powder on an Arcam A2 system (see Fig. 1). This artifact is commonly used by the EBM system developed for acceptance testing after system installation or major maintenance/reconfiguration operations.

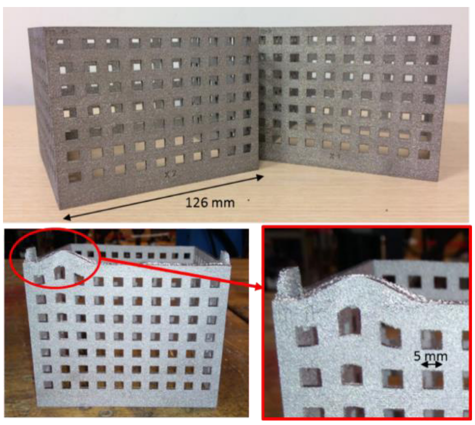


Fig. 1. Top panel: two in-control test parts produced via EBM; bottom panels: one out-of-control part produced via EBM and a detail of the local geometrical distortion

Fig. 1 (top panels) show two parts produced under in-control conditions, with acceptable final part quality. Fig. 1 (bottom panels) show one part produced with local geometrical defects caused by a wrong control of the powder recoating operation. All the parts were produced applying the nominal process parameters for the Ti6Al4V material (see Table 1).

Table 1. Detail information about the part, the material and the process parameters used in the real case study

| | |
|---|---|
| Part dimensions | 126 x 126 x 98,6 mm |
| Material | Ti6Al4V (size 45 – 106 μm) |
| Major process parameters | |
| Layer thickness | 50 μm |
| Max current | 20 mA |
| Focus offset | 25 mA |
| Speed function | 45 |
| Line offset | 0.2 mm |
| Hatch rotation | 90° |

Differently from laser-PBF systems, the Arcam A2 involves a feedback adaptation of the powder dosing in each layer. The recoated consists of a rake blade with metallic teeth that, under default settings, spreads the powder over the layer three times per layer. The powder is provided by two hoppers, on the left and on the right of the building area. On each side, a sensor measures a quantity that is a proxy of the amount of powder collected by the rake blade from the hopper. Depending on this sensor reading, the fetch positions of the rake are adapted layer-by-layer in order to keep a stable dosing from both the hopper during the entire process. When the sensor looses accuracy, the system may be forced to produce an over- or under-dosing, which leads to uneven powder beds and hence to local geometrical distortions (a.k.a. swelling) like the one shown in Fig. 1. The Arcam A2 system embeds different sensors that can be used to monitor the recoating process. Available signals for this purpose include the pulse values from powder flow sensors, the rake current and the rake positions.

In addition, the system embeds several other kinds of sensors for the measurement of temperature (at bottom level and column level), currents and voltages, beam current and focus, duration of each phase of the process, pressure levels, etc. In this study, we propose a statistical learning method for the monitoring of multiple signals associated to the powder recoating operation. The method can be extended to include a larger number of sensor readings into the monitoring tool to further enhance the embedded intelligence of the system.

## 3. Proposed methodology

In the presence of multivariate data from different sensors, data fusion techniques are needed to extract the relevant information content and, at the same time, tackle the violation of common assumptions adopted in statistical process control. Indeed, multi-sensor data typically exhibit violations of distributional assumptions that motivate the use of data mining / machine learning methods [40]. In this framework, a suitable technique for multi-sensor data fusion relies on the use of a one-class-classification variant of the Support Vector Machine (SVM) formalism. SVMs represent classification techniques based on the maximization of the margin between distinct classes. One-class-classification means that only one class is available for training, i.e. the class of in-control data, whereas any data point that does not belong to this class shall be classified as out-of-control. This variant, known as Support Vector Data Description (SVDD) [41 - 42] allows using the SVM method for statistical process monitoring. In the training phase, the SVDD algorithm is applied to a set of multivariate data representative of in-control conditions. First, a kernel width estimation is applied to determine the shape of a multivariate control region that adapts to the natural spread of the training data. Second, the kernel distance of each data point from the centre of the control region is computed and whenever such a distance is such that the data point is outside the control region, an alarm is issued. This monitoring scheme is also known as K-chart [41]. The analytic formulation of the SVDD procedure and the resulting monitoring scheme is briefly summarized in Appendix A.

The application of this method to the multi-sensor data gathered from embedded sensors during the EBM process works as follows:

- A training set consisting of in-control replicates of the same product is generated. For each part, the multi-sensor signals are recorded during the entire process.
- The SVDD control region is estimated based on training data. It can be used in retrospective way, to determine if the training data were actually in-control or not.
- During the production of new products, the sensor signals are acquired on-line and the corresponding values of the control statistic are compared with the designed control region. An alarm in case of control limit violation.

It is worth noticing that this approach applies to series production of the same product. Actually, most relevant industrial applications of the EBM process in the aerospace (e.g. turbine blades and fuel nozzles) and bio-medical sectors (e.g., hip prostheses and other medical implants) currently involve series production. However, it is known that one notable potential of metal additive manufacturing processes consists of being suitable for highly customized productions. In that case, a different training approach is needed. This can represent a possible extension of the current study.

## 4. Discussion of results

The proposed approach was applied to two sensor signals, i.e., the left and right rake sensor pulse signals. The pulse signal is a proxy of the amount of powder collected by the rake from one hopper. The left and right pulse signals during each powder recoating operation exhibit natural oscillations and varying gaps that depend on the natural variability of the powder dispatching process.

Fig. 2 shows an example of contours of the bivariate space spanned by the two sensor signals (training phase only) such that each contour corresponds to a Type I error, $\alpha$, value. The points plotted in Fig. 2 corresponds to measured sensor values during the production of in-control parts. Fig. 2 shows that the

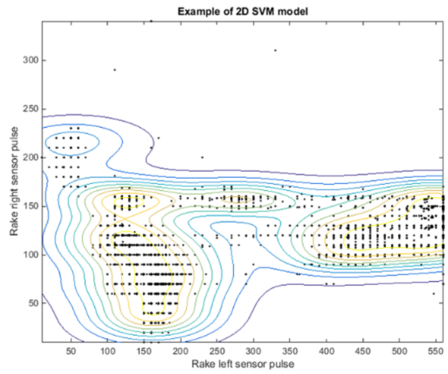


Fig. 2. Iso-lines of the SVDD control region corresponding to different Type I error levels (from bright yellow to dark blue in decreasing Type I error order); black points correspond to data observed during the training phase

bivariate distribution of the two signals is strongly non-normal and it exhibits some regions of the bivariate space where the density of measured values is higher. By setting $\alpha = 0.0027$, the control region is the one shown in Fig. 3. It was generated by applying a leave-one-out cross-validation to the training data.

Fig. 4 shows a superimposition of bivariate data acquired during the production of the two out-of-control parts (red points) superimposed to the training data and the SVDD control region. Fig. 4 shows that during the production of the out-of-control part there was a modification of the recoating

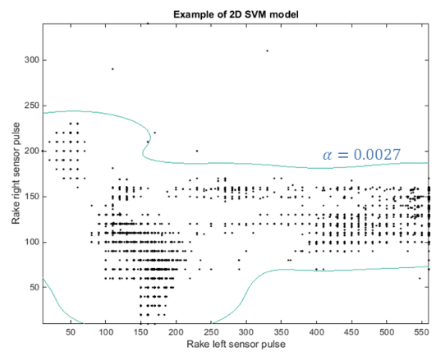


Fig. 3. SVDD control region corresponding to $\alpha = 0.0027$

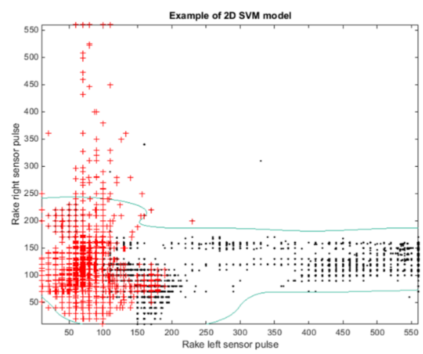


Fig. 4. Superimposition of bivariate data (red crosses) acquired during the production of the out-of-control part on the SVDD control region; black points correspond to bivariate signal data observed during the training phase

behavior. Indeed, the larger pulse peaks were observed on the right side instead of the left side, which probably caused a modification of the powder recoating and finally yielded the observed swelling effect.

Fig. 5 shows the time series of the right and left pulse signals acquired during the production of the out-of-control part. The red circles in the figure indicate the observations where an out-of-control was issued by the SVDD method. Fig. 5 shows that the anomalous recoating events occurred between layer 1050 and layer 1750, i.e., in the second half of the process. The analysis of the printed part shows a growing swelling effect starting from 70% of the overall height along the building direction.

An early detection of either an unexpected event or an out-of-control behavior provides the system with the novel capability of signaling an alarm during the production of the part and, when needed, of stopping the process. An early detection of deviations from the expected behavior is also fundamental to pave the way to the future development of novel strategies for in-line adaptation of process parameters and defect prevention/correction. The major advantage of the proposed method consists of using sensor data that are already available in the system, without the need to install additional and external sensing equipment.

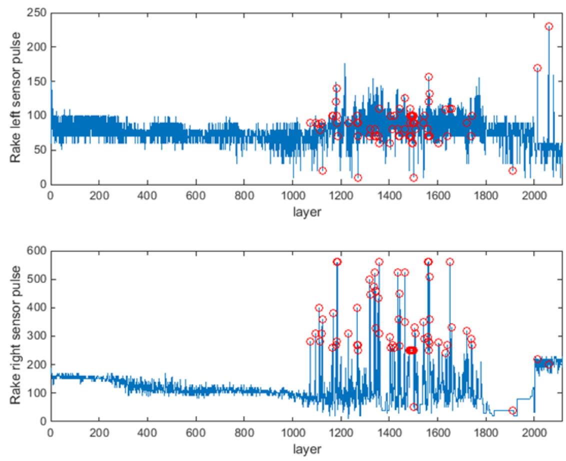


Fig. 5. Time series of the left (top panel) and right (bottom panel) sensor pulse signals acquired during the production of the out-of-control part; red circles indicate data points that were classified as out-of-control by the SVDD-based method.

## 5. Conclusion

The industrial breakthrough of PBF systems is still limited by quality related issues, especially in highly regulated sectors like the aerospace and biomedical ones, which are pulling the metal additive manufacturing market. Indeed, the stability and repeatability of process is affects by several sources of defects and process errors. Despite increasing efforts to integrate sensing toolkits in commercial PBF systems (mainly co-axial and off-axial cameras and pyrometers), there is still a lack of statistical methods to make sense of acquired data in-line and automatically detect the onset of defects. This study attempts to develop a novel data mining approach for EBM processes by using only sensor data that are already available in the system, i.e., sensors that are normally used for environmental control and for the normal management of process operations.

The study showed that the SVDD-based approach is suitable to learn from a training dataset representative of in-control process runs a control region that adapts to the natural spread of sensor data. The method can be used in-line to signal any major departure from the training pattern, to anticipate the detection of defects and faults and to enhance the embedded intelligence capabilities of the system.

The method here proposed can be extended in a future study to monitor a larger number of sensor signals, in order to expand the range of detectable defects and anomalous events.

## Appendix A. Support vector data description

Given a multivariate training dataset $\{\boldsymbol{x_j} \in \mathbb{R}^{\boldsymbol{p}}, \boldsymbol{j} = \boldsymbol{1}, \dots, \boldsymbol{M}\}$, where $\boldsymbol{x_j} = [\boldsymbol{x_{1,j}}, \boldsymbol{x_{2,j}}, \dots, \boldsymbol{x_{p,j}}]^{\boldsymbol{T}}$, the SVDD method consists of finding a minimal volume control region characterized by a centre $\boldsymbol{o} \in \mathbb{R}^{\boldsymbol{p}}$, and a radius $\boldsymbol{R}$, that can envelop a given percentage of the original data. The statistical process monitoring methods relies on the estimation of the kernel distance of any observation $\boldsymbol{z} \in \mathbb{R}^{\boldsymbol{p}}$ from the centre $\boldsymbol{o} \in \mathbb{R}^{\boldsymbol{p}}$ of that region. The control limit is estimated to guarantee a target Type I error with the available dataset. A kernel distance, hereafter denoted by $\boldsymbol{kd}(\boldsymbol{z})$, replaces the traditional Euclidean and statistical distance notions to adapt the control region boundary to the actual spread of the data. The estimation of the minimal volume control region, centred in $\boldsymbol{o} \in \mathbb{R}^{\boldsymbol{p}}$ and with radius $\boldsymbol{R}$, requires the solution of the following data-driven optimization problem:

$$\begin{aligned} &\min\left(R^2 + C\sum_{j=1}^{M}\xi_j\right) \\ &\text{s.t. } (\boldsymbol{x}_j - \boldsymbol{o})^T(\boldsymbol{x}_j - \boldsymbol{o}) \leq R^2 + \xi_j \text{ and } \xi_j \geq 0, \\ &j = 1, \dots, M \end{aligned} \tag{1}$$

where $\boldsymbol{\xi_j}, \boldsymbol{j} = \boldsymbol{1}, \dots, \boldsymbol{M}$, are slack variables, and $\boldsymbol{C}$ is a penalty coefficient used to weight the trade-off between the volume of the region and the percentage of enclosed data ($\boldsymbol{C} > \boldsymbol{0}$). By introducing the Lagrangian function:

$$\begin{aligned} L(R, \boldsymbol{o}, \xi_j; \alpha_j, \gamma_j) = R^2 + C\textstyle\sum_{j=1}^{M}\xi_j - \sum_{j=1}^{M}\alpha_j(R^2 + \xi_j - (\boldsymbol{x}_j \\ - \boldsymbol{o})^T(\boldsymbol{x}_j - \boldsymbol{o})) - \textstyle\sum_{j=1}^{M}\gamma_j\xi_j \end{aligned} \tag{2}$$

and by setting the partial derivatives w.r.t. $\boldsymbol{R}$, $\boldsymbol{o}$, and $\boldsymbol{\xi_j}, \boldsymbol{j} = \boldsymbol{1}, \dots, \boldsymbol{M}$, to zero, the problem (2) can be simplified as follows [41]:

$$\begin{aligned} &\max\left(\textstyle\sum_{j=1}^{M}\alpha_j\boldsymbol{x_j}^T\boldsymbol{x}_j - \sum_{j,k=1}^{M}\alpha_j\alpha_k\boldsymbol{x_j}^T\boldsymbol{x}_k\right) \\ &\text{s.t. } \textstyle\sum_{j=1}^{M}\alpha_j = 1 \text{ and } 0 \leq \alpha_j \leq C, j = 1, \dots, M \end{aligned} \tag{3}$$

A particularly interesting feature is that only the data points whose Lagrangian coefficients are larger than zero, called "support vectors", influence the shape of the region. This allows one not only to avoid the time-consuming estimation of the complete density function, but also to determine the shape of the control boundary by using a subset of original data.

By introducing the kernel trick, the inner product $\boldsymbol{a^T b}$ is replaced by a kernel function $\boldsymbol{K}(\boldsymbol{a} \times \boldsymbol{b})$. The kernel distance $\boldsymbol{kd}(\boldsymbol{z})$ of any new observation $\boldsymbol{z} \in \mathbb{R}^{\boldsymbol{p}}$ from the centre $\boldsymbol{o}$ is:

$$kd(\boldsymbol{z}) = K(\boldsymbol{z} \times \boldsymbol{z}) - 2\sum_{j=1}^{M} \alpha_j K(\boldsymbol{x}_j \times \boldsymbol{z}) + \sum_{j,k=1}^{M} \alpha_j \alpha_k K(\boldsymbol{x}_j \times \boldsymbol{x}_k) \quad (4)$$

In this study, the Gaussian radial basis (GRB) function was used and the heuristic procedure described in [41] for the kernel width selection was applied.

## References


[1] Mani M, Lane B, Donmez A, Feng S, Moylan S, Fesperman R. Measurement science needs for real-time control of additive manufacturing powder bed fusion processes. NIST Interagency/Internal Report (NISTIR), 8036, 2015.

[2] Sames WJ, List FA, Pannala S, Dehoff RR, Babu SS. The metallurgy and processing science of metal additive manufacturing. Int Mat Rev 2016; 1-46.

[3] Grasso M, Colosimo BM. Process Defects and In-situ Monitoring Methods in Metal Powder Bed Fusion: a Review, Meas Sc and Tech 2017; 28(4): 1-25.

[4] Thomas D. The development of design rules for selective laser melting (Doctoral dissertation, University of Wales), 2009

[5] Sharratt BM. Non-Destructive Techniques and Technologies for Qualification of Additive Manufactured Parts and Processes. A literature Review. Contract Report DRDC-RDDC-2015-C035, Victoria, BC, 2015.

[6] Craeghs T, Bechmann F, Berumen S, Kruth JP. Feedback control of Layerwise Laser Melting using optical sensors. Physics Procedia 2010; 5: 505-14.

[7] Craeghs T, Clijsters S, Kruth JP, Bechmann F, Ebert MC. Detection of process failures in layerwise laser melting with optical process monitoring. Physics Procedia 2012; 39: 753-9.

[8] Clijsters S, Craeghs T, Buls S, Kempen K, Kruth JP. In situ quality control of the selective laser melting process using a high-speed, real-time melt pool monitoring system. The International Journal of Advanced Manufacturing Technology 2014; 75(5-8): 1089-101.

[9] Lott P, Schleifenbaum H, Meiners W, Wissenbach K, Hinke C, Bültmann J. Design of an optical system for the in situ process monitoring of selective laser melting (LPBF). Physics Procedia 2011; 12: 683-90.

[10] Kruth JP, Mercelis P, Van Vaerenbergh J, Craeghs T. Feedback control of selective laser melting. In Proceedings of the 3rd international conference on advanced research in virtual and rapid prototyping 2007 p. 521-7.

[11] Yadroitsev I, Krakhmalev P, Yadroitsava I. Selective laser melting of Ti6Al4V alloy for biomedical applications: Temperature monitoring and microstructural evolution. Journal of Alloys and Compounds 2014; 583: 404-9.

[12] Doubenskaia M, Pavlov M, Grigoriev S, Tikhonova E, Smurov I. Comprehensive optical monitoring of selective laser melting. Journal of Laser Micro Nanoengineering 2012; 7(3): 236-43.

[13] Doubenskaia MA, Zhirnov IV, Teleshevskiy VI, Bertrand P, Smurov IY. Determination of true temperature in selective laser melting of metal powder using infrared camera. In Materials Science Forum 2015; 834: 93-102.

[14] Chivel Y. Optical in-process temperature monitoring of selective laser melting. Physics Procedia 2013; 41: 904-910.

[15] Pavlov M, Doubenskaia M, Smurov I. Pyrometric analysis of thermal processes in LPBF technology. Physics Procedia 2010; 5: 523-531.

[16] Kanko JA, Sibley AP, Fraser JM. In situ morphology-based defect detection of selective laser melting through inline coherent imaging. Journal of Materials Processing Technology 2016; 231: 488-500.

[17] Krauss H, Zeugner T, Zaeh MF. Layerwise monitoring of the selective laser melting process by thermography. Physics Procedia 2014; 56: 64-71.

[18] Lane B, Moylan S, Whitenton EP, Ma L. Thermographic Measurements of the Commercial Laser Powder Bed Fusion Process at NIST. In Proc. Solid Free. Fabr. Symp 2015; 575: 778-87.

[19] Bayle F, Doubenskaia M. Selective laser melting process monitoring with high speed infra-red camera and pyrometer. International Society for Optics and Photonics In Fundamentals of Laser Assisted Micro-and Nanotechnologies 2008; 6985.

[20] Schilp J, Seidel C, Krauss H, Weirather J. Investigations on temperature fields during laser beam melting by means of process monitoring and multiscale process modelling. Advances in Mechanical Engineering 2014; 6: 217584.

[21] Grasso M, Laguzza V, Semeraro Q, Colosimo BM. In-Process Monitoring of Selective Laser Melting: Spatial Detection of Defects Via Image Data Analysis. Journal of Manufacturing Science and Engineering 2017; 139(5), 051001-1 - 051001-16

[22] Repossini G, Laguzza V, Grasso M, Colosimo BM. On the use of spatter signature for in-situ monitoring of Laser Powder Bed Fusion, Additive Manufacturing 2017; 16: 35-48.

[23] Grasso M, Demir AG, Previtali B, Colosimo BM. In-situ Monitoring of Selective Laser Melting of Zinc Powder via Infrared Imaging of the Process Plume, Robotics and Computer-Integrated Manufacturing 2018; 49: 229-239.

[24] Jacobsmühlen J, Kleszczynski S, Schneider D, Witt G. High resolution imaging for inspection of laser beam melting systems. In 2013 IEEE International Instrumentation and Measurement Technology Conference (I2MTC) 2013; p. 707-12.

[25] Kleszczynski S, Zur Jacobsmühlen J, Sehrt JT, Witt G. Error detection in laser beam melting systems by high resolution imaging. In Proceedings of the Solid Freeform Fabrication Symposium 2012;2012

[26] Zhang B, Ziegert J, Farahi F, Davies A. In situ surface topography of laser powder bed fusion using fringe projection. Additive Manufacturing 2016; 12: 100-7.

[27] Foster BK, Reutzel EW, Nassar AR, Hall BT, Brown SW, Dickman CJ. Optical, layerwise monitoring of powder bed fusion. In Solid Free. Fabr. Symp. Proc 2015: 295-307.

[28] Land WS, Zhang B, Ziegert J, Davies A. In-situ metrology system for laser powder bed fusion additive process. Procedia Manufacturing 2015; 1: 393-403.

[29] Dunbar AJ. Analysis of the Laser Powder Bed Fusion Additive Manufacturing Process Through Experimental Measurement and Finite Element Modeling (Doctoral dissertation, The Pennsylvania State University) 2016.

[30] Everton SK, Hirsch M, Stavroulakis P, Leach R K, Clare AT. Review of in-situ process monitoring and in-situ metrology for additive manufacturing Materials and Design 2016; 95: 431-45;

[31] Gustavo T, Elwany A. A review on process monitoring and control in metal-based additive manufacturing J. Manufac. Sci. Eng. 2014; 136: 060801.

[32] Gong H. Generation and detection of defects in metallic parts fabricated by selective laser melting and electron beam melting and their effects on mechanical properties. UofL Electronic Theses and Dissertations 2013.

[33] Price S, Cooper K, Chou, K. Evaluations of temperature measurements by near-infrared thermography in powder-based electron-beam additive manufacturing. In Proceedings of the Solid Freeform Fabrication Symposium 2012: 761-73.

[34] Schwerdtfeger J, Singer RF, Körner C. In situ flaw detection by IR-imaging during electron beam melting. Rapid Prototyping Journal 2012; 18(4): 259-263.

[35] Ridwan S, Mireles J, Gaytan SM, Espalin D, Wicker RB. Automatic layerwise acquisition of thermal and geometric data of the electron beam melting process using infrared thermography. In Proc. Int. Symp. Solid Freeform Fabrication 2014; 343.

[36] Rodriguez E, Medina F, Espalin D, Terrazas C, Muse D, Henry C, ... Wicker RB. Integration of a thermal imaging feedback control system in electron beam melting. In Proceedings of the Solid Freeform Fabrication Symposium, 2012.

[37] Rodriguez E, Mireles J, Terrazas C et al.. Approximation of absolute surface temperature measurements of powder bed fusion additive manufacturing technology using in situ infrared thermography. Additive Manufacturing 2015; 5: 31-9.

[38] Mireles J, Terrazas C, Gaytan SM, Roberson DA, Wicker RB. Closed-loop automatic feedback control in electron beam melting. The International Journal of Advanced Manufacturing Technology 2015; 78(5-8): 1193-9.

[39] Tax DMJ, Duin RPW. Support Vector Data Description, Machine Learning 2004; 54: 45-66

[40] Grasso M, Colosimo BM, Semeraro Q, Pacella M. A Comparison Study of Distribution-Free Multivariate SPC Methods for Multimode Data. Quality and Reliability Engineering International 2015; 31(1): 75-96

[41] Ning X, Tsung F. Improved Design of Kernel Distance-Based Charts Using Support Vector Methods, IIE Transactions 2013; 45(:), 464-76

[42] Tax DMJ. One-Class Classification; Concept-Learning In The Absence Of Counter-Examples, Ph.D. thesis, Delft University of Technology, 2001